Invited Paper

Scaling of the microwave and dc conductance of metallic single-walled carbon nanotubes

Zhen Yu, Chris Rutherglen, Peter J. Burke
Integrated Nanosystems Research Facility, Department of Electrical Engineering and Computer Science, University of California, Irvine, CA 92697-2625

ABSTRACT

We measure the dynamical conductance of electrically contacted single-walled carbon nanotubes at dc and ac as a function of source-drain voltage in both low and high dc bias voltage. We show a direct relationship between the ac conductance and dc conductance. We also measure the microwave conductance of 2 nanotubes in parallel and observe an anomalous frequency dependence.

Keywords: Nanotube, nanotechnology.

1. INTRODUCTION

Because of their superior transport properties, including conductivities larger than copper[1], single-walled carbon nanotubes are possible candidates as interconnects in either all-nano or hybrid silicon-nano integrated circuits. An issue that has not been experimentally addressed in any detail is the high-speed performance of carbon nanotubes as interconnects. In this work, we measure the frequency dependent microwave properties of individual, electrically contacted metallic single-walled carbon nanotubes.

In recent work, we measured the dynamical conductivity of metallic SWNTs as a function of dc source-drain bias from dc to 10 GHz[2]. In this work, we extend those measurements to other devices and present a scaling relationship between the dc and ac conductance for individual metallic SWNTs. We also present RF data on two nanotubes in parallel.

2. FABRICATION

Our samples were grown by CVD using methods described in [3]. Individual SWNTs were synthesized via chemical vapor deposition[4] on oxidized, p-doped Si wafers with a 300-400 nm SiO_2 layer. Metal electrodes were formed on the SWNTs using electron-beam lithography and metal evaporation of a 30-nm Pd/20-nm Cr/100 nm Au trilayer[5]. Nanotubes with electrode spacing of 1 µm were studied. Figure 1 shows an SEM image of device A. Figure 2 shows an SEM image of device B, which has two metallic CNTs in parallel.

Nanostructure Integration Techniques for Manufacturable Devices, Circuits, and Systems: Interfaces, Interconnects, and Nanosystems, edited by Freund, Islam, Dutta
Proc. of SPIE Vol. 6003, 60030Q, (2005) · 0277-786X/05/$15 · doi: 10.1117/12.631867

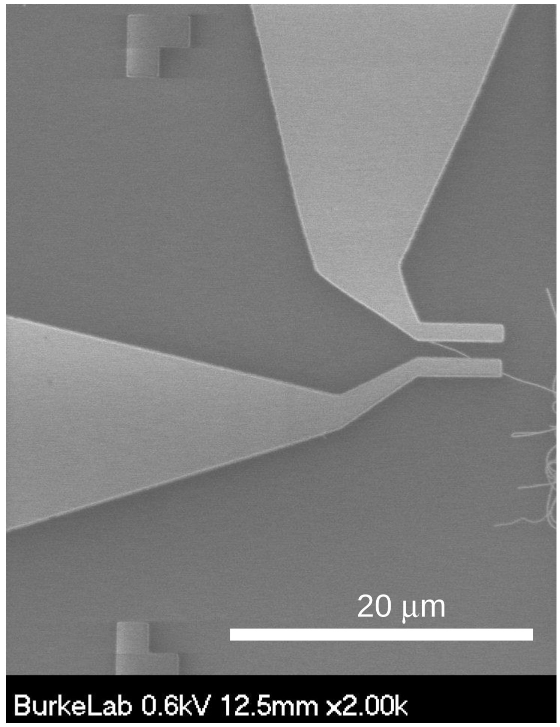

Fig. 1: SEM image of device A.

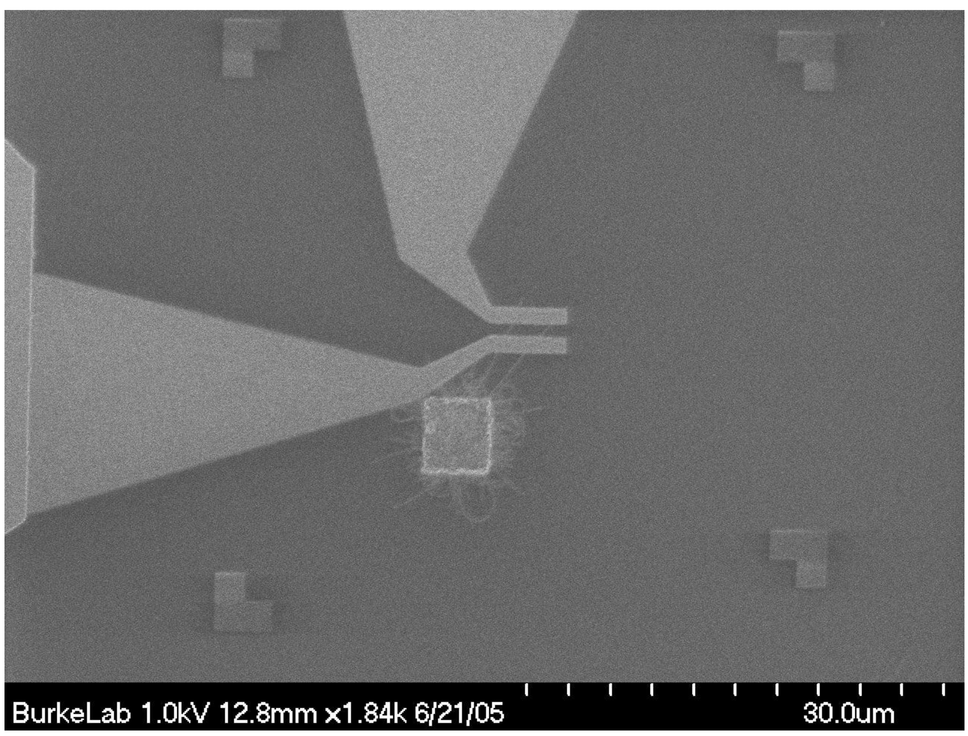

Fig. 2: SEM image of device B.

3. MEASUREMENT CALIBRATION

Our measurements are performed at room temperature in air. We use a network analyzer and a one-port measurement technique to measure the microwave power reflected off of an electrically contacted, individual metallic single-walled nanotube. To measure the dynamical impedance at microwave frequencies, a commercially available microwave probe (suitable for calibration with a commercially available open/short/load calibration standard) allowed for transition from coax to lithographically fabricated on chip electrodes. A microwave network analyzer is used to measure the calibrated (complex) reflection coefficient $S_{11}(\omega) \equiv V_{reflected}/V_{incident}$, where $V_{incident}$ is the amplitude of the incident microwave signal on the coax, and similarly for $V_{reflected}$. This is related to the load impedance $Z(\omega)$ by the usual reflection formula: $S_{11}=[Z(\omega)-50\ \Omega]/[Z(\omega)+50\ \Omega]$. At the power levels used, the results are independent of the power used.

As we discussed in quantitative detail in our recent work[2], measurements of the absolute value of the microwave conductance of a high impedance device are generally associated with significant error bars. This is because of the difficulty in separating the inherent device performance from parasitics in parallel with the device. Unless extreme care is taken in the calibration, these parasitics are difficult to model and hence “calibrate out”. However, *changes* in the device ac properties with dc bias are much clearer since the dc bias can be changed without the need to physically adjust the probes. This assumes that the parasitics do not change with dc bias, which can easily be checked in a control experiment. In our experience, such control experiments are critical since in certain cases the doped semiconducting substrate can change its rf feedthrough properties depending on the electrode dc bias, which can easily be mistaken for intrinsic nanotube performance.

By linearizing the relationship between S_{11} and the conductance G, it can be shown that for small values of G (compared to 50 Ω), G(mS) ≈ 1.1 x S_{11}(dB). In this paper, we use this relationship. As discussed in our recent work[2], the resistive impedance is so large that it is very difficult to determine the reactive impedance.

4. INDIVIDUAL TUBE RESULTS AND DISCUSSIONS

4.1. DC properties

Fig. 3 shows the room temperature I-V characteristic of device A with a 1 μm source-drain spacing. Since this length is comparable to the mean-free-path, this device is in the quasi-ballistic limit at low bias, but in the diffusive regime at high bias. The low-bias resistance of this device was 65 kΩ. This resistance is most likely predominantly due to the contact; at low fields, once electrons are injected, transport is quasi-ballistic from source to drain. The device clearly shows saturation in the current at around 25 μA, consistent with our prior devices[2] and other work[6].

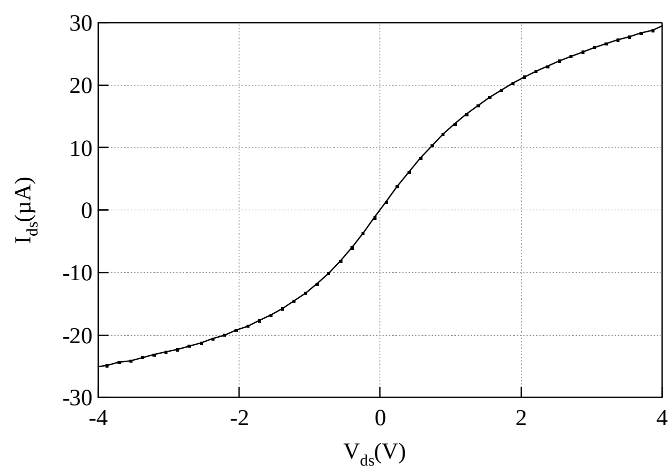

Fig.3: I-V characteristic of device A.

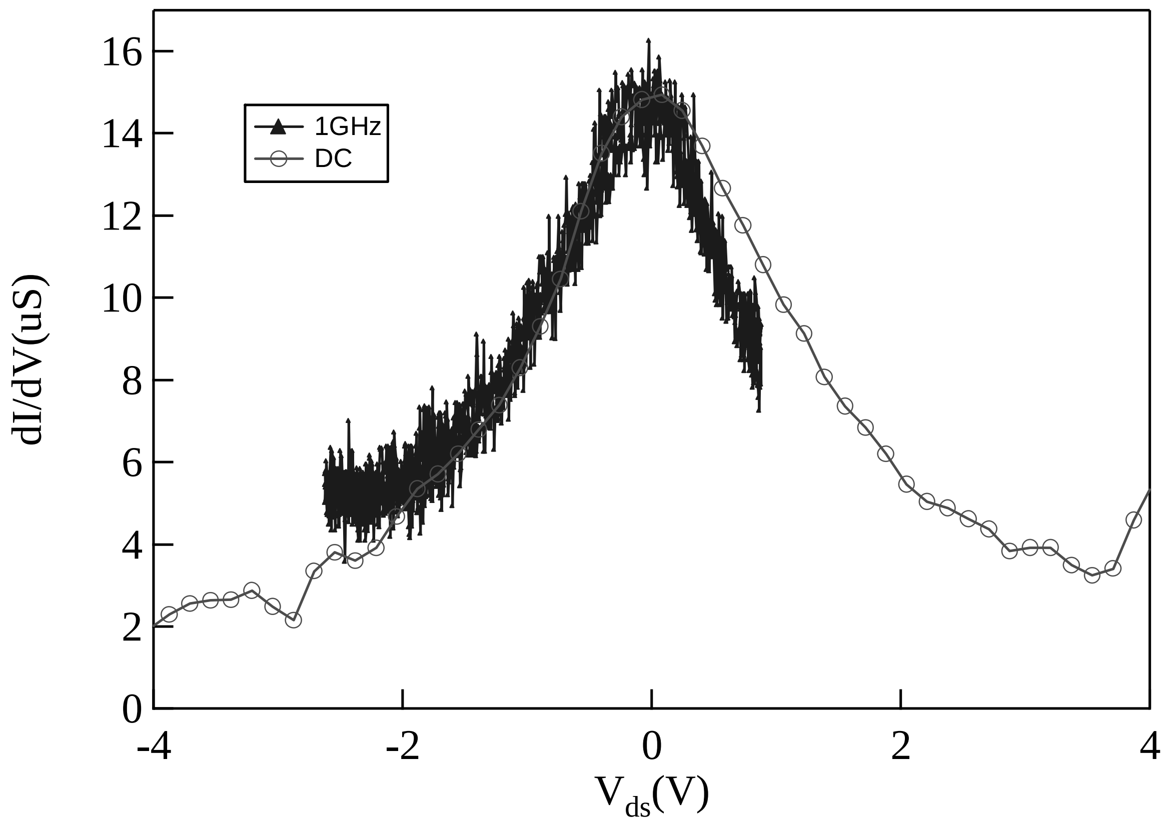

Fig. 4: Small signal conductance vs. source-drain voltage at dc and 1 GHz for device A.

4.2. AC properties

In fig. 4, we plot the dc dynamical conductance determined by numerically differentiating the dc I-V curve. We also plot the ac conductance at 1 GHz, using the formula $\Delta G(\text{mS}) \approx 1.1 \times \Delta S_{11}(\text{dB})$. We have added an offset to the ac conductance to be normalized to the dc conductance, as discussed in ref. [2] in depth. It can be seen that the ac conductance changes with dc source-drain voltage just as the dc conductance does for this device. We next turn to this trend for this device, and two other recently published devices[2].

5. SCALING OF AC CONDUCTANCE WITH DC CONDUCTANCE

We now to the question of whether the dc and ac conductance are correlated. In Fig. 5, we plot the change in the dc conductance vs. the change in the ac conductance when the source-drain voltage is varied over the same range. The data are device A from this paper, and devices from our recent paper[2]. It is clear from this data that the dc and ac conductance changes with source-drain voltage in the same way, regardless of the device on resistance, over the range studied. The range studied includes devices with conductance up to 0.1 x 4 e^2/h. An interesting study for future work will be to determine if this trend holds for devices up to conductance of order 4 e^2/h.

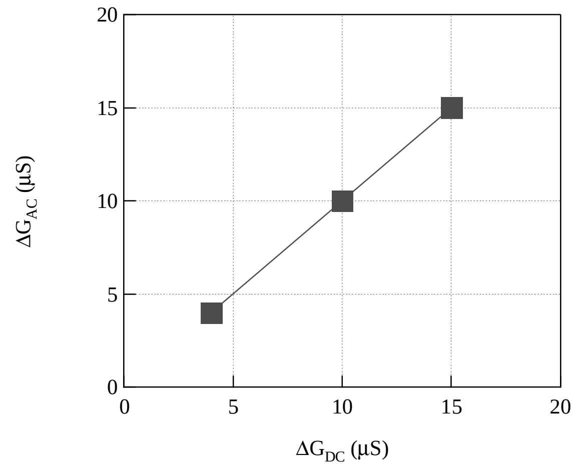

Fig. 5: ΔG at ac vs. ΔG at dc (i.e. change in small signal conductance with V_{ds}) for different individual CNT devices.

6. PARALLEL TUBES

6.1. DC properties of two metallic nanotubes in parallel

Fig. 3 shows the room temperature I-V characteristic of device B with a 1 μm source-drain spacing. There are two metallic CNTs in parallel. The low-bias resistance of this device was 16 kΩ. The device clearly shows saturation in the current at around 50 μA. The current carrying capability increased because of two CNTs in parallel. Interestingly, this device shows negative differential resistance at around 2 V. In addition, there is a suppression of the conduction at the origin. At present neither of these interesting phenomenon that we observe are understood.

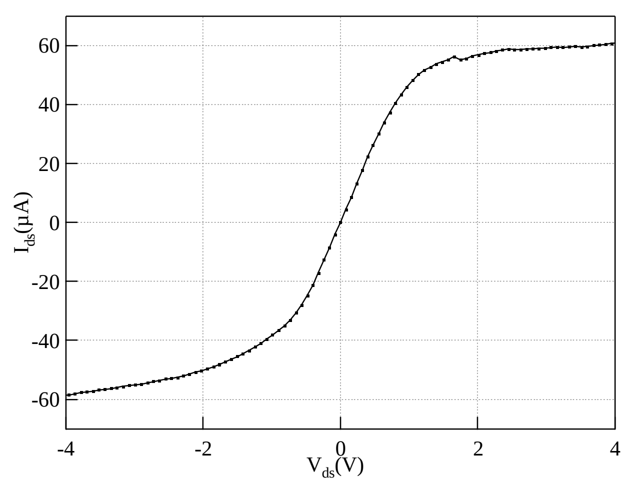

Fig.6 : I-V characteristic of device B, which has two metallic nanotubes in parallel.

6.2. AC properties of two metallic nanotubes in parallel

In fig. 7, we plot the dc dynamical conductance determined by numerically differentiating the dc I-V curve. We also plot the ac conductance at 1 GHz, using the formula $\Delta G(mS) \approx 1.1 \times \Delta S_{11}(dB)$. We have added an offset to the ac conductance to be normalized to the dc conductance at high dc source drain bias. (This offset was also independently determined using a control sample on the same wafer with no nanotubes). It can be seen that the ac conductance changes with dc source-drain voltage by and amount different than the dc conductance does for this device. In fact, this seems to indicate suppression in the high frequency conductance at low bias, as seen in the figure. At present, this perplexing result is not understood. This is the first time that the impedance of a nanotube has been demonstrated to depend on frequency. In this case, the frequency dependence is measured at only two frequencies: dc and 1 GHz. An important project for future research will be to more carefully measure this frequency dependence and to elucidate its physical origin.

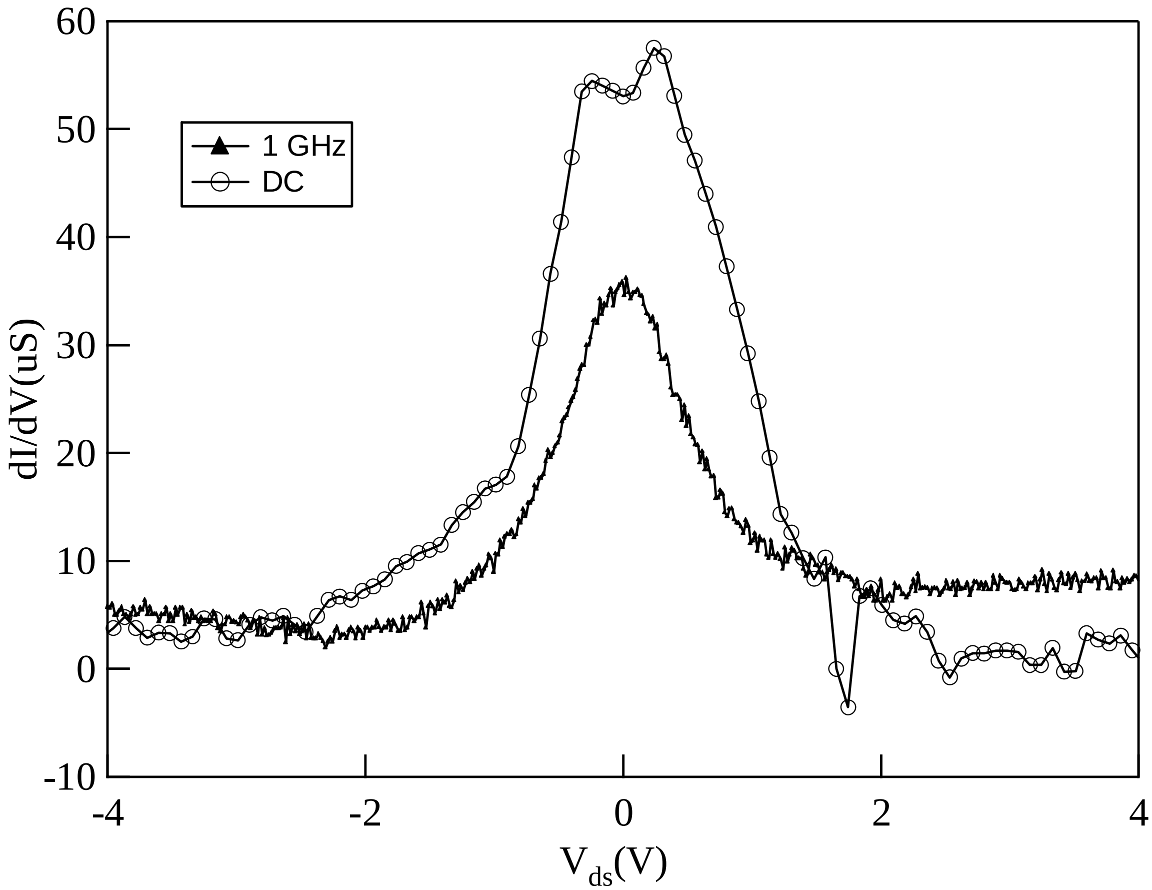

Fig. 7: Small signal conductance vs. source-drain voltage at dc and 1 GHz for device B (two nanotubes in parallel.)

7. CONCLUSIONS

We have measured the dynamical conductance of electrically contacted single-walled carbon nanotubes at dc and ac as a function of source-drain voltage in both low and high dc bias voltage. We showed a direct relationship between the ac conductance and dc conductance. We also measured the microwave conductance of 2 nanotubes in parallel and observed an anomalous frequency dependence.

ACKNOWLEDGEMENTS

This work was supported by the Army Research Office (award DAAD19-02-1-0387), the Office of the Naval Research (award N00014-02-1-0456), , and the National Science Foundation (award ECS-0300557, CCF-0403582, DMR-0216635).

REFERENCES

[1.] S. D. Li, Z. Yu, C. Rutherglen and P. J. Burke, "Electrical Properties of 0.4 Cm Long Single-Walled Carbon Nanotubes", *Nano Letters*, **4**, 2003-2007, (2004).

[2.] Z. Yu and P. J. Burke, "Microwave Transport in Metallic Single-Walled Carbon Nanotubes", *Nano Letters*, **5**, 1403-1406, (2005).

[3.] Z. Yu, S. D. Li and P. J. Burke, "Synthesis of Aligned Arrays of Millimeter Long, Straight Single-Walled Carbon Nanotubes", *Chemistry of Materials*, **16**, 3414-3416, (2004).

[4.] J. Kong, H. T. Soh, A. M. Cassell, C. F. Quate and H. J. Dai, "Synthesis of Individual Single-Walled Carbon Nanotubes on Patterned Silicon Wafers", *Nature*, **395**, 878-881, (1998).

[5.] A. Javey, J. Guo, Q. Wang, M. Lundstrom and H. J. Dai, "Ballistic Carbon Nanotube Field-Effect Transistors", *Nature*, **424**, 654-657, (2003).

[6.] Z. Yao, C. L. Kane and C. Dekker, "High-Field Electrical Transport in Single-Wall Carbon Nanotubes", *Physical Review Letters*, **84**, 2941-2944, (2000).